Separation Science and Technology
Publication details, including instructions for authors and subscription information:
http://www.informaworld.com/smpp/title~content=t713708471

Constant Surface Charge Model in Floc Foam Flotation. The Flotation of Copper(II)

Tony E. Chatman[a]; Shang-Da Huang[a]; David J. Wilson[a]
[a] DEPARTMENT OF CHEMISTRY, VANDERBILT UNIVERSITY, NASHVILLE, TENNESSEE

To cite this Article Chatman, Tony E. , Huang, Shang-Da and Wilson, David J.(1977) 'Constant Surface Charge Model in Floc Foam Flotation. The Flotation of Copper(II)', Separation Science and Technology, 12: 4, 461 — 484
To link to this Article: DOI: 10.1080/00372367708058090
URL: http://dx.doi.org/10.1080/00372367708058090

SEPARATION SCIENCE, 12(4), pp. 461–484, 1977

Constant Surface Charge Model in Floc Foam Flotation. The Flotation of Copper(II)

TONY E. CHATMAN, SHANG-DA HUANG, and DAVID J. WILSON*

DEPARTMENT OF CHEMISTRY
VANDERBILT UNIVERSITY
NASHVILLE, TENNESSEE 37235

Abstract

Cu(II) is effectively floated from synthetic mixtures and industrial waste samples by floc foam floatation using $Fe(OH)_3$ and sodium lauryl sulfate at pH's of approximately 6.5. The separation becomes marginal at ionic strengths above 0.25 [residual Cu(II) concentrations greater than 1 ppm]. A constant surface charge model for floc foam flotation is found to result in less effective binding than the constant surface potential model.

INTRODUCTION

The foam flotation literature has been recently reviewed by Lemlich (*1*), and Somasundaran (*2, 3*). The work of Zeitlin's group on adsorbing colloid flotation (*5–7*), particularly Kim's study of the flotation of copper(II) from seawater (*8*) with ferric hydroxide and dodecylamine at pH 7.6, is relevant to our present study. We have previously used ferric hydroxide with sodium lauryl sulfate (NLS) to remove lead(II) (*9*) and cadmium(II) (*10*); a number of other adsorbing colloid flotation separations are described in our recent report (*11*). A. J. Rubin and Johnson (*12*),

*To whom requests for reprints should be sent.

Talbot and Dick (*13*), Sebba (*14*), and Huang and Wilson (*10*) have carried out work on the ion or precipitate flotation of copper(II).

We have used the Gouy-Chapman picture (*15*) of the electric double layer in the calculation of the adsorption isotherms of floc particles on ionic surfactant films within the frameworks of a number of physical models. These include a cell model (*16*), a cell model with floc-floc screening (*17*), a cluster integral approach (*18*), and a model including hemimicelle formation (*19*). Previously Jorné and E. Rubin had used Gouy-Chapman theory to explain the effects of ionic size and charge on the selectivity of foam fraction (*20*).

We present here data on the adsorbing colloid flotation of copper(II) with ferric hydroxide and NLS. Effects of pH and ionic strength are examined. We then examine the application of Gouy-Chapman theory to the comparison of the interaction of plane parallel interfaces having (a) fixed surface potentials of opposite sign, and (b) fixed surface charge densities of opposite sign.

FLOC FOAM FLOTATION OF COPPER(II). APPARATUS AND CHEMICALS

Two flotation systems were utilized. Figure 1 depicts the apparatus used for the batch separations; the column was made of Pyrex glass tubing and was 3.5 cm in diameter by 90 cm in length. The pH of the solution being foamed was continuously monitored by means of a microcombination electrode which was mounted in a ground glass joint on a sidearm 12 cm from the bottom of the column. The bottom of the column was closed by means of a large rubber stopper in which were mounted a stopcock for sample collection, a drain to facilitate rapid emptying and flushing of the column, and a 40–60 mesh fine pore fritted glass sparger for introducing the air which generated the foam. Two small holes in this stopper permitted insertion of tygon tubing from a 10-ml syringe (used to inject surfactant) and a 1-ml syringe (used to inject either dilute nitric acid or sodium hydroxide to adjust the pH before and during a run). Foam was discharged from a sidearm 4 cm from the top of the column; foam was caught and collapsed in a beaker to determine the volume of foamate generated during a run.

The flow of house air through the fritted glass sparger was controlled by a microvalve with vernier control; flow rates were measured with a soap film flowmeter and stopwatch. The air was passed through ascarite to remove acidic gases (such as CO_2), through a water saturater, and

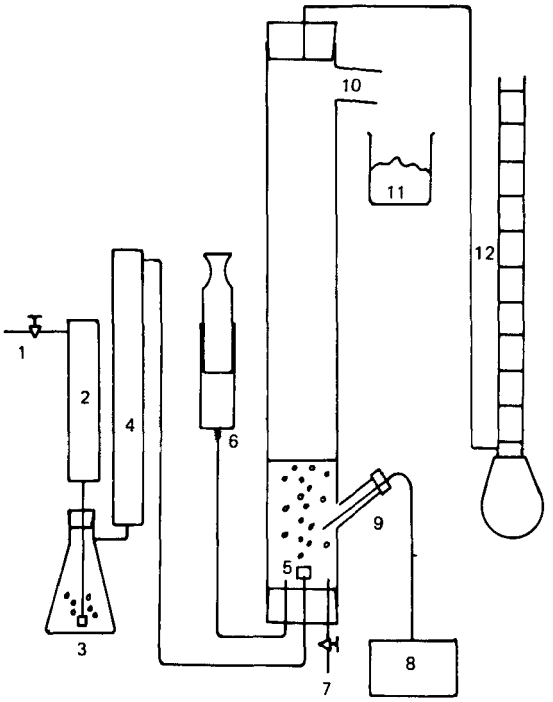

FIG. 1. The batch apparatus.

1:	air needle valve	7:	drain
2:	ascarite tube for CO_2 removal	8:	pH meter
3:	humidifier	9:	pH electrode port
4:	glass wool column	10:	foam discharge port
5:	fritted glass sparger	11:	discharged foam
6:	reagent syringe	12:	soap film flowmeter

through a 2 × 50 cm column packed with glass wool to remove dusts or mists.

The continuous flow column shown in Fig. 2 was of Pyrex glass, 5 cm diameter by 121 cm in length. A sidearm 5 cm from the top permitted discharge of the foam to a rotating wire spider foam breaker; a second sidearm 50 cm from the bottom of the column was fitted with a ground joint and housed a microcombination electrode for monitering the pH of the contents of the column. The bottom of the column was closed with a large stopper in which were mounted a fritted glass gas sparging tube, the effluent drain, and the influent line. The level of the liquid pool at the

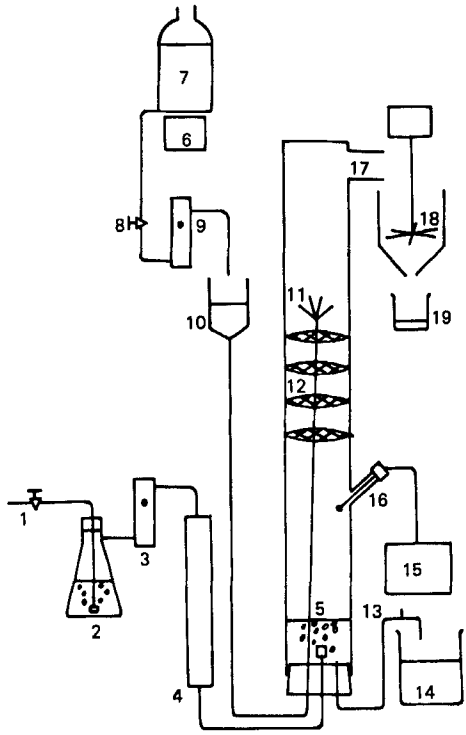

FIG. 2. The continuous flow apparatus.

1:	air needle valve	11:	influent dispersion head
2:	humidifier	12:	foam baffles
3:	air flowmeter	13:	effluent drain
4:	glass wool column	14:	effiuent
5:	fritted glass sparger	15:	pH meter
6:	magnetic stirrer	16:	pH electrode port
7:	influent reservoir	17:	foam discharge port
8:	influent valve	18:	foam breaker
9:	influent flowmeter	19:	collapsed foamate
10:	constant head reservoir		

bottom of the column was controlled by adjusting the height of a vent in the Tygon tubing used for the effluent drain. Effluent was collected in a calibrated bottle to permit determination of flow rates. The influent port in the base of the column housed a 75-cm glass tube 8 mm in diameter which carried influent to a small dispersion head located approximately 65 cm from the base of the column. The dispersion head was made of a short piece of copper tubing, closed at the top end; four smaller pieces of copper tubing were mounted at right angles to each other and at an angle of 45° above the horizontal. The ends of these smaller tubes were closed, and 4 small holes were drilled in each. This dispersion head greatly improved the uniformity of flow over that obtained with an earlier head, and increased the effective volume of foam actually being utilized for separation.

Four wire screen baffles 3 cm apart were mounted in the column approximately 45 to 57 cm from its base; these stabilized the foam, reducing turbulence and foam upset. Horizontal placement of the screens was quite critical, as was their diameter. A screen which fit too tightly to the glass walls or was placed at an angle to the horizontal tended to create turbulence and channeling in the foam.

A reservoir for containing the sample solution, floc, and surfactant was mounted close to the top of the column. A magnetic stirrer in this reservoir prevented settling out of the floc. Sample flow was regulated by a pinch clamp on the tubing leading from the base of the sample reservoir to a 0 to 100 cc/min flowmeter which then discharged to the influent line. The air flow rate was controlled in the same manner as in the batch apparatus, except that a 0 to 0.5 l/min flowmeter was used to moniter airflow in addition to the soap film flowmeter. House air was humidified and passed through glass wool.

Laboratory grade NLS was used as collector because of its effectiveness in this separation, low cost, and ready availability. A stock solution containing 1000 ppm of NLS in distilled water was prepared; this was discarded 2 weeks after being made up to avoid problems with bacterial growth in the surfactant. Certified ACS grade cupric nitrate was used to prepare a 1000 ppm aqueous Cu(II) solution; 10 ml of concentrated nitric acid was added per liter of solution to prevent possible surface adsorption of copper to the polyethylene containers. Aliquots of stock solution were diluted volumetrically and acidified with nitric acid to provide standard solutions for use in the atomic absorption analysis of copper. Certified ACS grade ferric nitrate and sodium hydroxide were used to prepare the ferric hydroxide flocs; a 1000-ppm solution of ferric ion was prepared from

ferric nitrate and distilled water, and 1.0 and 0.1 *M* solutions of sodium hydroxide were made up. Certified ACS grade sodium nitrate, sodium sulfate, sodium hydroxide, and reagent grade nitric acid were used to adjust the ionic strength and pH of the solutions being foamed. Atomic absorption analysis of the effluent from the flotation columns to which all the above chemicals had been added except cupric nitrate indicated no detectable copper.

A Sargent-Welch Model LSX pH meter with a microcombination electrode was used to adjust and moniter pH in both the batch and the continuous flow studies. Conductivity measurements on some industrial wastewater samples were made on a YSI conductivity bridge. Copper concentrations were measured on a Perkin-Elmer Model 305B atomic absorption spectrophotometer at 324.7 nm.

EXPERIMENTAL PROCEDURES

Batch foaming runs were carried out as follows. Appropriate aliquots of the stock solutions of cupric nitrate and ferric nitrate were diluted to between 100 and 150 ml with distilled water and 1 *M* sodium nitrate solution added to bring the ionic strength of the final solution to the desired level. The pH was adjusted by addition of 1 *M* sodium hydroxide initially; final adjustment was made by addition of 0.1 *M* sodium hydroxide and 0.1 *M* nitric acid. The solution was continuously stirred during the precipitation of the ferric hydroxide (pH range 3 to 4) and final adjustment of pH. The solution was then diluted to volume (190 ml), poured into the column, and aeration begun. An air flow rate of 60 ml/min was used; this led to a relatively dry foam and yielded separations which were essentially complete in less than half an hour. The pH, which tended to drift to higher values during the course of the runs, was adjusted from time to time during the run by addition of small quantities of nitric acid from the syringe provided for that purpose. This upward drift in pH is probably due to both the sparging of CO_2 from the solution and the foam fractionation of hydrogen ion from the solution by the anionic surfactant. In our earlier runs all 10 ml of surfactant was added at the beginning of the run; more efficient separations and more stable foams were obtained by adding 5 ml of surfactant at the beginning of the run and 5 ml more 6 min later. [A number of workers have noted the advantage of this distributed addition of surfactant (*21–23*).]

Five milliliter samples were withdrawn from the column at 5 min intervals; the sampling stopcock was purged just before each sample was

taken. The sample was acidified (1 drop of 8 *M* nitric acid) to prevent adsorption of copper to the sample bottle. In a few runs the remaining solution in the column was acidified (pH 2.2) at the end of the run, mixed, and a sample taken to demonstrate that no significant amount of copper was adsorbing to the glass column.

Continuous flow experiments were carried out on both synthetic solutions and copper smelter wastewaters. The desired aliquot of copper stock solution or industrial waste was placed in a 3-liter beaker, the copper stock solution diluted to nearly 2 liters, and ferric nitrate added. The pH was then adjusted to the desired level, NLS added, and the solution diluted to 2.0 liters with distilled water. (Very little dilution was used with the industrial waste samples.) The solution was then poured into the sample reservoir, from which the sample flow into the column was regulated at a flow rate of roughly 50 ml/min. The column was initially primed by the addition of 40 ml of 1000 ppm NLS solution to establish a column of foam; the air flow rate was maintained at 200 ml/min. Excessive sample flow rates resulted in channeling, overturning of the foam, and drastic deterioration in column performance. The level of liquid in the bottom of the column was controlled by adjusting the height of the raffinate discharge tube; samples were taken from this tube at 5 min intervals and acidified with nitric acid before atomic absorption analysis.

DATA AND CONCLUSIONS

Effect of pH and Ionic Strength on Rate and Extent of Separation

Hydrogen ion and OH^- are generally potential-determining ions for oxides and hydroxide; the isoelectric point for $Cu(OH)_2$ has been reported as 7.6 and 9.4 (*24*). The isoelectric points for $Fe(OH)_3$ given in this reference range from pH 6.0 to 8.5, depending upon the composition and history of the system; Mattson and Pugh report an isoelectric point of 7.1 for $Fe(OH)_3$ in water (*25*). One would anticipate that separations with anionic surfactants like NLS would be ineffective at pH's above about 7; the solubility product of $Cu(OH)_2$, 1.6×10^{-19} (*26*), suggests that a pH of 8.5 would be necessary to reduce the copper(II) concentration to 1 ppm, making separation impossible. Apparently, however, the activity of $Cu(OH)_2$ coprecipitated with or adsorbed on $Fe(OH)_3$ is substantially less than that of pure $Cu(OH)_2$, inasmuch as Table 1 shows that quite good separations are obtained at pH's as low as 6.0 if the ionic strength is low. At pH's above 8 the rate of floc removal is quite slow; at pH's

TABLE 1

Floc Foam Flotation of Copper with $Fe(OH)_3$ and NLS[a]

	Residual copper (ppm)							
	Added $NaNO_3$ (M)							
pH	0	0.025	0.050	0.075	0.10	0.15	0.25	0.50
5.5	3.0	6.4	7.2	6.2	5.5	>13	>13	>13
6.0	0.10	0.37	0.61	1.4	2.7	1.0	6.5	>13
6.5	0.02	0.11	0.17	0.17	0.17	0.28	1.5	>13
7.0	0.02	0.11	0.07	0.06	0.22	2.8	1.1	>13
7.5	0.01	0.07	0.13	0.55	1.4	13.1	5.2	>13
8.0	0.02	0.10	0.77	0.71	>13	>13	>13	>13

[a]All runs made with 50 ppm Cu(II), 100 ppm Fe(III), and 50 ppm NLS (25 ppm initially, 25 ppm 5 min after the start of the run). Initial volume = 200 ml, air flow rate = ~60 ml/min, duration of runs = 25 min.

below about 6.5 the copper is not removed effectively on the floc, although the floc itself is rapidly removed. With no added $NaNO_3$ and at pH 8.5, 0.35 ppm of Cu(II) remained in solution; at pH 9.0, >5.4 ppm of Cu(II) remained.

We were interested in attempting to extend this method to solutions of somewhat higher ionic strength. We therefore modified the technique as follows. To 200 ml samples containing 50 ppm Cu(II) was added 225 ppm Fe(III), and the pH adjusted to the desired level. The solution was placed in the foaming column and 50 ppm NLS added; another 25 ppm NLS was added after 6 min. Fe(III) stock solution to provide another 25 ppm

TABLE 2

Copper Separations at High Ionic Strength—Improved Method[a]

Ionic strength	pH	Rate of removal of $Fe(OH_3)$	Residual Cu(II) (ppm)
0.50	5.5	Medium	>13
	6.0	Slow	3.80
0.35	6.0	Slow	2.95
	6.5	Slow	4.72
0.25	6.5	Slow	0.67
	7.0	Very slow	9.1
0.20	6.5	Slow	0.43

[a]Initial Cu(II) concentration 50 ppm; air flow rate 60 ml/min; residual Cu(II) determined after 25 min of treatment.

and NLS stock solution to provide another 25 ppm were mixed, neutralized to the desired pH, and added to the sample after 11 min. Samples for analysis were withdrawn after 25 min; the results are indicated in Table 2, and indicate significant but not spectacular improvement.

Effects of Fe(III) and NLS Concentrations

In these separations one wishes to minimize expenses for surfactant and floccing chemicals without, however, jeopardizing the separation. A number of runs were therefore made with pH adjusted to roughly the optimal value (6.5), 50 ppm Cu(II), ionic strengths in the range observed in several industrial waste samples, 50 ppm NLS initially followed by 25 ppm at 6 min and 25 ppm at 11 min. The results are given in Table 3, and indicate that roughly 150 ppm of Fe(III) is needed to efficiently remove 50 ppm of Cu(II).

The extent to which copper removal is achieved by adsorption, as contrasted to coprecipitation, was determined qualitatively by precipitating the floc, placing it in the column and adjusting its pH to the desired

TABLE 3

Effect of Fe(III) Concentration upon Cu(II) Removal

Ionic strength (moles/l)	Volume of Fe(III) added (ml)[a]	Total Fe(III) concentration (ppm)	Residual Cu(II) (ppm)
0.025	40 + 10	250	0.11
	20 + 10	150	0.66
	20 + 5	125	2.01
	10 + 5	75	0.55
	10 + 2.5	62.5	1.20
0.050	40 + 10	250	0.17
	40 + 5	225	0.28
	30 + 10	200	0.21
	30 + 5	175	0.27
	20 + 10	150	0.16
	20 + 5	125	0.93
	10 + 10	100	1.68
	10 + 5	75	1.19
	5 + 5	50	1.31
	5 + 2.5	37.5	1.38

[a]The first number is the volume of Fe(III) stock solution added at the beginning of the run; the second, the volume added with the final NLS addition after 11 min. Conditions in these runs were as in Table 2, except for Fe(III) concentration.

TABLE 4

Mode of Cu(II) Removal[a]

Sample no.	Residual Cu(II) (ppm)	
	Copper added after precipitation of $Fe(OH)_3$	Copper added before precipitation of $Fe(OH)_3$
1	14.1	3.1
2	11.0	2.4
3	10.3	2.3
4	9.8	2.1
5	9.8	2.1

[a]The Fe(III), Cu(II), and NLS concentrations were initially 75, 50, and 50 ppm, respectively. The Fe(III) was all added initially; NLS was added in 3 portions of 10, 5, and 5 ml of the 1000-ppm stock solution. The pH was 6.5 and the ionic strength was 0.05 (adjusted with $NaNO_3$). Initial sample volume was 200 ml, the duration of treatment was 25 min, and air flow rate was 60 ml/min.

TABLE 5

Effect of NLS Concentration on Cu(II) Removal[a]

Total NLS concentration (ppm)[b]	Volume of NLS added (ml)[c]	Residual Cu(II) (ppm)
100	10 + 5 + 5	0.17
75	5 + 5 + 5	0.34
50	5 + 2.5 + 2.5	0.38
37.5	5 + 2.5 + 0	0.31
25	5 + 0 + 0	0.39
12.5	2.5 + 0 + 0	0.39
5	1 + 0 + 0	2.01

[a]Initial concentrations of Fe(III) and Cu(II) were 200 and 50 ppm; an additional 50 ppm of $Fe(OH)_3$ was added after 11 min. Ionic strength = 0.05 mole/l; pH = 6.5, and air flow rate = 60 ml/min.

[b]These are the concentrations that would have been present initially if all the NLS had been added initially.

[c]These numbers give the volumes of NLS stock solution added at 0, 6, and 11 min after the start of the run.

level, adjusting the pH of the Cu(II) solution to the desired level, and adding the Cu(II) and NLS solutions to the column. A comparison of runs of this type with runs made in which coprecipitation occurred is shown in Table 4. It is evident that coprecipitation permits the reduction of Cu(II) concentrations to levels well below those which can be achieved by adsorption (with simultaneous occurrence, presumably, of ion flotation).

The effect of varying the NLS concentration is shown in Table 5. In these runs the initial Fe(III) and Cu(II) concentrations were 200 and 50 ppm respectively; an additional 50 ppm of Fe(III) was added after 11 min. The pH was held at 6.5, and the ionic strength was 0.05 *M*. The figures in the column labeled "Volume of NLS added" refer to the volumes of NLS stock solution (1000 ppm) added to the sample at 0, 6, and 11 min after the start of the run. Samples were taken for analysis after 25 min of treatment. At the lowest NLS concentration the foam was sparse and unstable, and the level of separation attained was unacceptable.

In some runs the floc was permitted to remain in contact with the solution for periods up to 5 hr before foaming. No additional copper was removed after the first half hour.

Industrial Waste Samples

Four copper-containing industrial wastewater samples were obtained in the course of this study; the characteristics of these samples are summarized in Table 6. Several batch techniques were used on Sample no. 1 which resulted in separations but did not reduce Cu(II) levels in the waste to the target figure of 0.3 ppm; the following method, however, was capable of meeting this criterion. Initially 200 ppm of Fe(III) and 50 ppm of NLS were added to the waste and the pH was adjusted to the desired

TABLE 6

Characteristics of Industrial Wastewater Samples

Sample no.	pH	Total dissolved solids (g/l)	Conductivity (μmho/cm)	Ionic strength[a]	Cu(II) (ppm)
1	2.38	1.30	3.34×10^3	0.039	188
2	6.35	1.24	4.85×10^2	0.005	23.5
3	6.25	1.48	4.98×10^2	0.005	5.8
4	6.50	1.13	5.65×10^2	0.005	50

[a]Calculated as Na_2SO_4 from the conductivity.

TABLE 7

Batch Separations of Industrial Samples[a]

Sample no.	Initial Cu(II) (ppm)	pH	Residual Cu(II) (ppm)
1	100	7.0	0.06
			0.00
			0.19
			0.19
2	17.6	5.0	7.8
		5.5	1.1
		6.0	0.33
		6.5	0.23
		7.0	7.5
3	4.33	5.0	0.55
		5.5	0.14
		6.0	0.00
		6.5	0.04
		7.0	3.7
		7.0	1.3
4	29.9	6.0	0.31
		6.5	0.09
		7.0	0.17
		7.5	1.37

[a]Consult text for procedure.

value. The solution volume at this point was about 200 ml. Foaming was initiated (air flow rate of approximately 60 ml/min), and 25 ppm of NLS was added after 6 min. After 11 min another 25 ppm of NLS and 50 ppm of Fe(III) were added; the pH of the added solution was adjusted to the desired level. Samples were taken for analysis after 25 min of foaming. As is seen in Table 7, this method was able to reduce the Cu(II) concentration to or below the target figure in all of these waste samples. A pH of 6.5 appears to be optimal.

Continuous Flow Studies

The results of the batch studies encouraged us to carry out work on the continuous flow apparatus as the first stage in scaling up to industrial-size equipment. Two-liter synthetic samples containing 200 ppm Cu(II) as cupric nitrate were prepared; to these were added 4 or 8 g/l of Na_2SO_4 and the desired amount of Fe(III) as ferric nitrate. The pH was then adjusted with NaOH solution, and the NLS stock solution (1 g/l) was added.

At the beginning of the run 40 ml of the NLS stock solution was added directly to the column in order to establish the foam. Data from one of the early runs are given at the top of Table 8. It was found that careful placement and fitting of screen baffles below the influent dispersion head and careful vertical alignment of the column decreased channeling and axial dispersion in the stripping section of the column. These modifications resulted in the next two runs listed in Table 8. We note that the high ionic strengths and high copper(II) concentrations of these synthetic mixtures are substantially in excess of what we had felt could be treated by floc

TABLE 8

Continuous Flow Runs, Synthetic Mixtures[a]

Run	Sample no.	pH	Added Na_2SO_4 (g/l)	Effluent Cu(II) (ppm)
1	1	6.5	8.0	0.35
	2			0.94
	3			1.27
	4			1.27
	5			1.33
	6			1.44
	7			1.44
	8			1.53
	9			1.52
2	1	7.0	4.0	0.16
	2			0.24
	3			0.32
	4			0.42
	5			0.60
	6			0.57
	7			0.76
	8			0.65
3	1	6.5	4.0	0.33
	2			0.35
	3			0.28
	4			0.23
	5			0.24
	6			0.34
	7			0.30
	8			0.39

[a]Air flow rate = 200 ml/min; sample flow rate = 50 ml/min; sample volume = 2000 ml; NLS concentration = 75 ppm; Cu(II) concentration = 200 ppm; Fe(III) concentration = 400 ppm. The column was primed with 40 ml of NLS stock solution to establish the foam.

TABLE 9

Continuous Flow Studies of Industrial Wastewater Samples[a]

Waste sample no.	Sample volume (ml)	Initial Cu(II) (ppm)	pH	Aliquot no.	Effluent Cu(II) (ppm)
1	2000	82.2	6.5	1	0.26
				2	0.20
				3	0.35
				4	0.46
				5	0.53
				6	0.54
				7	0.47
				8	0.47
				9	0.56
				10	0.45
2	2000	23.5	6.5	1	0.06
				2	0.07
				3	0.03
				4	0.03
				5	0.06
				6	0.12
				7	2.72
				8	0.07
				9	0.06
				10	0.07
				11	0.04
3	1250	5.8	6.0	1	0.07
				2	0.02
				3	0.05
				4	0.04
				5	0.04
				6	0.03
				7	0.05
4	2000	49.8	6.0	1	0.08
				2	0.12
				3	0.11
				4	0.08
				5	0.12
				6	0.14
				7	0.16
				8	0.12
				9	0.20
				10	0.16
				11	0.14
				12	0.14

[a]See text for concentrations of reagents, flow rates, etc.

foam flotation, and represent a rather stringent test of the method. At an air flow rate of 200 ml/min, approximately 15% of the liquid is carried over as foamate; in industrial operation this would be clarified and recycled to avoid waste of surfactant. The excessive wetness of the foam was due at least in part to a column design which did not allow sufficient time for foam drainage.

The industrial wastewater samples were treated with 400 ppm Fe(III), 150 ppm NLS (plus 40 ml of NLS stock solution to prime the column), and foamed at an air flow rate of 200 ml/min and an influent flow rate of approximately 50 ml/min. Sample no. 1, nearly exhausted by previous runs, was diluted somewhat to yield a volume of 2000 ml; as run, it contained 82 ppm Cu(II). The results are listed in Table 9, and establish the ability of the method to produce effluents containing quite low levels of copper from industrial wastewaters. One would expect that the amount of iron(III) used could be markedly reduced for those wastewaters containing relatively little copper(II) without significant impairment of the separation.

CONSTANT SURFACE POTENTIAL AND CONSTANT CHARGE MODELS OF FLOC FOAM FLOTATION

The equilibrium values of surface potentials are completely determined by the compositions of the pairs of phases involved (*27*), and are not dependent on the geometrical configurations of the systems involved. In our earlier work we have therefore assumed that the surface potentials ψ_1 (of the air–water interface) and ψ_2 (of the floc–water interface) are independent of the distance between these two interfaces, and that the surface charges are able to change with changing configuration sufficiently rapidly to maintain the equilibrium values of ψ_1 and ψ_2. Now it is quite conceivable that this transport of charge carriers has a sufficiently high free energy of activation that it is much slower than can be equilibrated during the approach time of an encounter between the two surfaces. If so, then one might better consider the surface charge densities as constant, rather than the surface potentials. The constant surface charge model is also the appropriate one when the charge of the surface is determined by the dissociation of groups fixed at the surface, such as SO_3H groups on sulfonated coal (*27*).

We here compare some aspects of the constant surface potential and the constant surface charge density models. We take as our system two

large plane parallel surfaces of opposite surface charge immersed in an electrolyte solution.

CONSTANT SURFACE CHARGE MODEL

Consider the system having fixed surface charge densities σ_1(negative) and σ_2 (positive), separated by a distance l. Poisson's equation for the system is

$$\frac{d^2\psi}{dx^2} = -\frac{4\pi\rho}{D} = \frac{8\pi e N_0 c_\infty}{D} \sinh\left(\frac{e\psi}{kT}\right) \tag{1}$$

where ψ = electric potential a distance x from the surface charge density σ_1
ρ = charge density
D = dielectric constant of water
e = |electronic charge|
N_0 = Avogadro's number
c_∞ = concentration of 1–1 electrolyte, in equivalents/cm^3
k = Boltzmann's constant
T = absolute temperature

The equation can be integrated to yield (*15*)

$$\frac{d\psi}{dx} = \left\{\left(\frac{\partial\psi}{\partial x}\right)_1^2 + 2\left(\frac{kT}{ea}\right)^2\left[\cosh\frac{e\psi}{kT} - \cosh\frac{e\psi_1}{kT}\right]\right\}^{1/2} \tag{2}$$

where

$$\left|\left(\frac{\partial\psi}{\partial x}\right)_1 = \frac{\partial\psi}{\partial x}\right|_{x=x_1}$$

and

$$a^2 = \frac{DkT}{8\pi e^2 N_0 c_\infty}$$

Integration of Eq. (2) yields

$$\int_{\psi_1}^{\psi(x)} \frac{d\psi}{\left\{\left(\frac{\partial\psi}{\partial x}\right)_1^2 + 2\left(\frac{kT}{ea}\right)^2\left[\cosh\frac{e\psi}{kT} - \cosh\frac{e\psi_1}{kT}\right]\right\}^{1/2}} = x \tag{3}$$

The relation between surface charge density σ_n and surface potential

ψ_n is given by

$$\sigma_n = (-1)^n \frac{D}{4\pi}\left(\frac{d\psi}{dx}\right)_n, \qquad n = 1, 2 \tag{4}$$

Evaluating Eq. (4) at $x = x_2$ yields

$$\left(\frac{d\psi}{dx}\right)_2 = \left\{\left(\frac{d\psi}{dx}\right)_1^2 + 2\left(\frac{kT}{ea}\right)^2\left[\cosh\frac{e\psi_2}{kT} - \cosh\frac{e\psi_1}{kT}\right]\right\}^{1/2} \tag{5}$$

We rearrange Eq. (5) to obtain

$$\left\{\left[\left(\frac{d\psi}{dx}\right)_2^2 - \left(\frac{d\psi}{dx}\right)_1^2\right]\Big/2\left(\frac{kT}{ea}\right)^2\right\} + \cosh\frac{x\psi_1}{kT} \equiv w = \cosh\frac{e\psi_2}{kT} \tag{6}$$

$$\psi_2 = \frac{kT}{e}\operatorname{argcosh} w \tag{7}$$

Thus ψ_2 is expressed in terms of knowns σ_1 and σ_2, and unknown ψ_1, from Eqs. (4), (6), and (7). The unknown ψ_1 is then calculated by Newton's method from Eq. (8), which is obtained by setting $x = l$, $\psi(x) = \psi_2$ in Eq. (3):

$$l = \int_{\psi_1}^{\psi_2} \frac{d\psi}{\left\{\left(\frac{d\psi}{dx}\right)_1^2 + 2\left(\frac{kT}{ea}\right)^2\left[\cosh\frac{e\psi}{kT} - \cosh\frac{e\psi_1}{kT}\right]\right\}^{1/2}} \tag{8}$$

The resulting value of ψ_1 is then used in Eq. (3) to generate x as a function of ψ over the range (ψ_1, ψ_2).

We now examine the problem of calculating the free energy of the system.

During the interaction, no charge is transferred from one phase to another, so the chemical part of the contribution to the free energy of the potential-determining ions is constant and can be ignored. The free energy is then simply the work necessary to charge the double layer in a reversible way starting from zero charge. The charges of the potential-determining ions are imagined to be transported gradually from infinity to the surfaces. After each increment of charge the ions in solution are allowed to reequilibrate, during which no work is done, so the free energy of the process is given by

$$G(l) = \int_0^{\sigma_1}\left(\psi_1' + \frac{\sigma_2}{\sigma_1}\psi_2'\right)d\sigma_1' \tag{9}$$

where ψ_1' and ψ_2' are the surface potentials at x_1 and x_2 when the two

surfaces are separated by a distance l and charged to charge densities of σ'_1 and $\sigma_2\sigma'_1/\sigma_1 = \sigma'_2$, respectively. For given values of σ'_1 and σ'_2 the corresponding values of ψ_1 and ψ_2 are calculated from Eqs. (4) through (8), permitting (rather laborious) numerical evaluation of the integral in Eq. (9).

The free energy at infinite separation is also given by Eq. (9), except that ψ'_1 and ψ'_2 are evaluated when $l = \infty$. The free energy of interaction of the two surfaces is given by

$$V(l) = G(l) - G_\infty \tag{10}$$

CONSTANT SURFACE POTENTIAL MODEL

The free energy per unit area of a system composed of two large parallel surfaces separated by a distance l and immersed in electrolyte solution is (*15*, *28*)

$$G(l) = -2N_0c_\infty kT\int_0^l\left[\cosh\frac{e\psi}{kT} - 1\right]dx - \frac{D}{8\pi}\int_0^l\left(\frac{d\psi}{dx}\right)^2 dx \tag{11}$$

The corresponding free energy when the two surfaces are at infinite separation is

$$G_\infty = -8N_0c_\infty kTa\left[\cosh\frac{e\psi_1}{kT} + \cosh\frac{e\psi_2}{kT} - 2\right] \tag{12}$$

The free energy of interaction per cm^2 of the two surfaces is then given by Eq. (10), as before.

RESULTS

Plots of $V(l)$ vs l at various concentrations of 1–1 electrolyte are shown in Fig. 3 for the constant surface potential model; these check our previous results (*28*). As noted before, decreasing the ionic strength very markedly increases both the range and the magnitude of the attractive interaction. Figure 4 shows the dependence of surface charge density $\sigma_2(l)$ on separation distance l at various ionic strengths; σ_2 increases drastically with decreasing l, as one would anticipate. At an ionic strength of 2×10^{-7} mole/cm^3, σ^2 varies from 5.59×10^2 esu/cm^2 at $l = \infty$ to 1.04×10^5 esu/cm^2 at $l = 2$ Å, a 200-fold increase. At an ionic strength of 10^{-3} mole/cm^3, the surface charge increases by a factor of about 3, from 3.96×10^4 to 1.10×10^6 esu/cm^2 as l goes from ∞ to 2 Å.

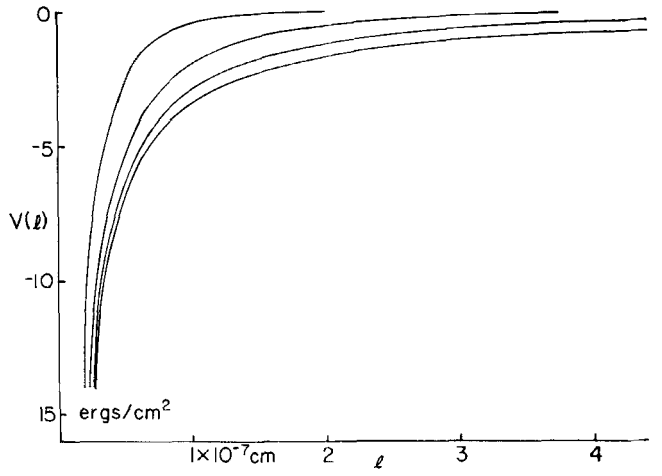

FIG. 3. Dependence of $V(l)$ on ionic strength, constant surface potential model. $\psi_1 = -50$ mV; $\psi_2 = 50$ mV; $T = 298°$K (in all figures); $D = 78.5$ (in all figures); $c_\infty = 10^{-3}$, 10^{-4}, 10^{-5}, and 2×10^{-7} mole/cm^3 (top to bottom).

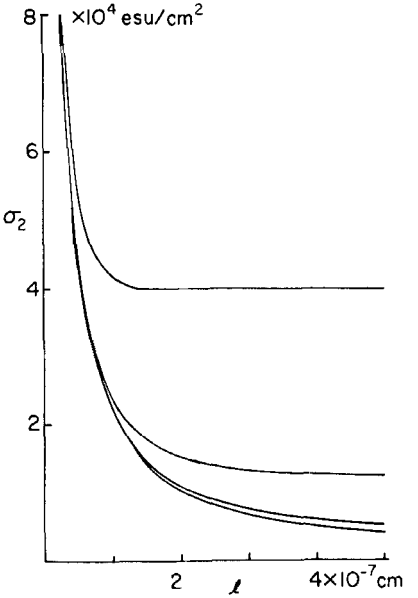

FIG. 4. Dependence of surface charge density σ_2 on distance of separation l and salt concentration. All parameters as in Fig. 3; $c_\infty = 10^{-3}$, 10^{-4}, 10^{-5}, and 2×10^{-7} mole/cm^3 from top to bottom.

The dependence of $V(l)$ upon the surface potentials is shown in Fig. 5; in these plots $\psi_1 = -\psi_2$. In Fig. 6 we see the dependence of surface charge density $\sigma_2(l)$ on surface potential. As expected, the surface charge density and the interaction potential both increase in magnitude with increasing magnitude of surface potentials.

We now turn to the constant surface charge density model. Figures 7, 8, and 9 show the electric potentials between the two surfaces for $l = 300$, 100, and 10 Å, respectively. The ionic strength was 10^{-5} mole/cm^3 and

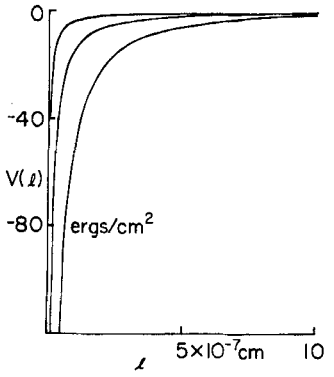

FIG. 5. Dependence of $V(l)$ on surface potentials, constant surface potential model. ψ_1 and ψ_2, $\psi_2 = -\psi_1 = 50$, 100, and 200 mV (top to bottom); $c_\infty = 10^{-6}$ mole/cm^3.

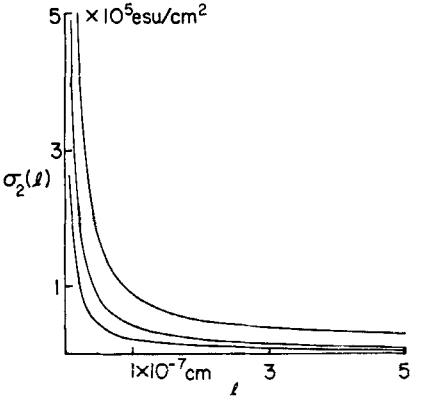

FIG. 6. Variation of σ_2 with l and surface potentials. $\psi_2 = -\psi_1 = 50$, 100, and 200 mV (bottom to top); $c_\infty = 10^{-6}$ mole/cm^3.

$-\sigma_1 = \sigma_2 = 4 \times 10^3$ esu/cm^2 in all cases. The magnitude of the potential decreases and the ψ vs l plots approach linearity as the two surfaces are brought closer together.

Plots of ψ_1 vs l for solutions of varying ionic strength are shown in Fig. 10. The magnitude of the surface potential increases with decreasing ionic strength, and we note that in this model the surface potentials approach zero when the surfaces approach each other sufficiently closely

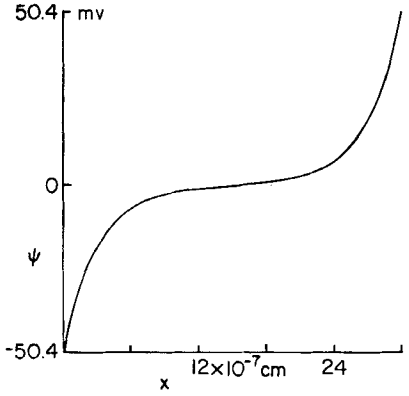

FIG. 7. Electric potential between two surfaces, constant surface charge density model. $-\sigma_1 = \sigma_2 = 4.0 \times 10^3$ esu/cm^2; $c_\infty = 10^{-5}$ mole/cm^3; $l = 3.0 \times 10^{-6}$ cm.

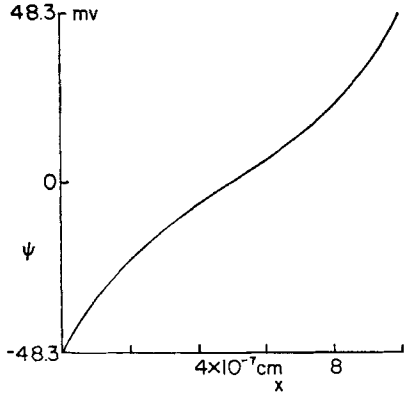

FIG. 8. Electric potential between two surfaces. All parameters as in Fig. 7, except $l = 1.0 \times 10^{-6}$ cm.

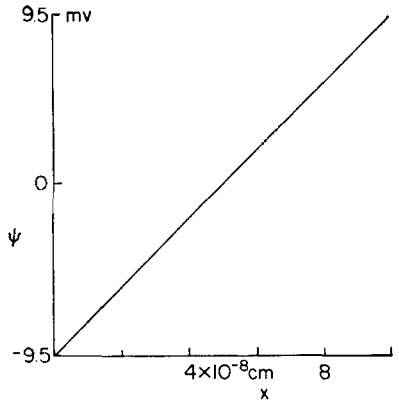

FIG. 9. Electric potential between two surfaces. All parameters as in Fig. 7, except $l = 1.0 \times 10^{-7}$ cm.

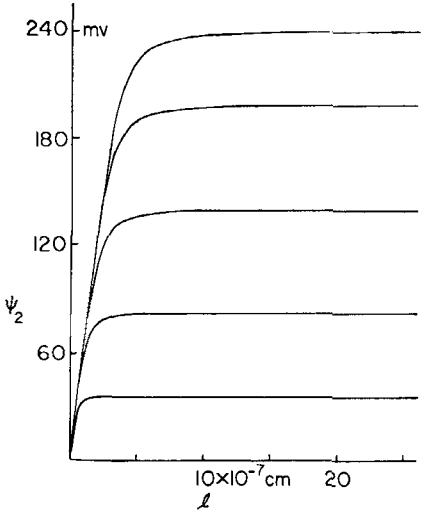

FIG. 10. Dependence of ψ_2 on l and c_∞, constant surface charge density model. $-\sigma_1 = \sigma_2 = 2.6 \times 10^4$ esu/cm^2; $c_\infty = 2 \times 10^{-7}$, 10^{-6}, 10^{-5}, 10^{-4}, and 10^{-3} mole/cm^3 from top to bottom.

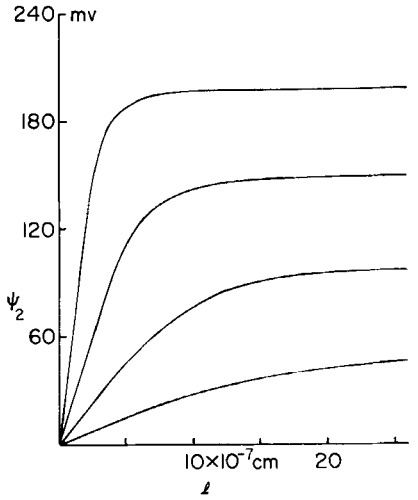

FIG. 11. Dependence of ψ_2 on l and surface charge density. $c_\infty = 10^{-6}$ mole/cm^3; $-\sigma_1 = \sigma_2 = 2.60 \times 10^4$, 1.01×10^4, 3.76×10^3, and 1.25×10^3 esu/cm^2 from top to bottom; $\psi_2(\infty) = 200$, 150, 100, and 50 mV from top to bottom.

if $\sigma_1 = -\sigma_2$. The range of the interaction between the two surfaces is seen to increase with decreasing ionic strength, as with the constant surface potential model. Figure 11 exhibits plots of ψ_1 vs l at several constant surface charge densities. Somewhat surprisingly, the surface potential starts to decrease significantly only at lower l for higher surface charge densities.

The free energy of interaction for the constant surface charge model was not evaluated because of the substantial amount of computer time which would have been required. Nevertheless, we can draw a qualitative conclusion from the facts that the magnitudes of the surface potentials decrease as the two surfaces approach and that decreasing the magnitudes of the surface potentials in the constant potential model decreases the magnitude of $V(l)$ at fixed l. Let us compare two models having the same values of ψ_1 and ψ_2 when $l = \infty$. As l decreases, the decreasing magnitudes of ψ_1 and ψ_2 for the constant charge density model will result in a smaller binding energy $|V(l)|$ than would be obtained with the constant surface potential model. The constant surface charge model would thus be expected to yield substantially less efficient floc adsorption isotherms

than a constant surface potential model having the same measured surface potentials of the air–water and floc–water interfaces.

Acknowledgment

This work was supported by the Environmental Protection Agency under Grant No. R-803564.

REFERENCES

1. R. Lemlich (ed.), *Adsorptive Bubble Separation Techniques*, Academic, New York (1972).
2. P. Somasundaran, *Sep. Purif. Methods*, *1*, 117 (1972).
3. P. Somasundaran, *Sep. Sci.*, *10*, 93 (1975).
5. D. Voyce and H. Zeitlin, *Anal. Chim. Acta*, *69*, 27 (1974).
6. F. Chaine and H. Zeitlin, *Sep. Sci.*, *9*, 1 (1974).
7. C. Matsuzaki and H. Zeitlin, *Ibid.*, *8*, 185 (1973).
8. Y. S. Kim and H. Zeitlin, *Ibid.*, *7*, 1 (1972).
9. R. P. Robertson, D. J. Wilson, and C. S. Wilson, *Sep. Sci.*, *11*, 569 (1976).
10. S.-D. Huang and D. J. Wilson, *Ibid.*, *11*, 215 (1976).
11. D. J. Wilson, *Foam Flotation Treatment of Heavy Metals and Fluoride-Bearing Industrial Wastewaters*, U.S. Environmental Protection Agency Report.
12. A. J. Rubin and J. D. Johnson, *Anal. Chem.*, *39*, 298 (1967).
13. F. D. Talbot and W. L. Dick, *Ind. Eng. Chem., Fundam.*, *10*, 309 (1971).
14. F. Sebba, U.S. Patent 3,476,553 (1969).
15. E. J. W. Verwey and Th. G. Overbeek, *Theory of the Stability of Lyophobic Colloids*, Elsevier, Amsterdam, 1948.
16. J. W. Wilson, D. J. Wilson, and J. H. Clarke, *Sep. Sci.*, *11*, 223 (1976).
17. D. J. Wilson, *Ibid.*, *11*, 389 (1976).
18. D. J. Wilson, *Ibid.*, *12*, 231 (1977).
19. D. J. Wilson, *Ibid.*, *12*, 447 (1977).
20. J. Jorné and E. Rubin, *Ibid.*, *4*, 313 (1969).
21. R. B. Grieves and T. E. Wilson, *Nature*, *205*, 1066 (1965).
22. K. A. Razumov, G. V. Illyuvieva, and T. F. Poltoranina, *Obogashch. Rud.*, *10*, 14 (1965).
23. R. B. Grieves and D. Bhattacharya, *J. Appl. Chem.*, *19*, 115 (1969).
24. G. A. Parks, *Chem. Rev.*, *65*, 177 (1965).
25. S. Mattson and A. J. Pugh, *Soil Sci.*, *38*, 299 (1934).
26. T. R. Hogness, W. C. Johnson, and A. R. Armstrong, *Qualitative Analysis and Chemical Equilibrium*, Holt, Rinehart, and Winston, New York, 1966, p. 565.
27. J. Th. G. Overbeek, in *Colloid Science*, Vol. 1 (H. R. Kruyt, ed.), Elsevier, Amsterdam, 1952, Chap. 6.
28. J. W. Wilson and D. J. Wilson, *Sep. Sci.*, *9*, 381 (1974).

Received by editor November 5, 1976